

A REVERSE-SHOCK MODEL FOR THE EARLY AFTERGLOW OF GRB 050525A

L. SHAO AND Z. G. DAI

Department of Astronomy, Nanjing University, 22 Hankou Lu, Nanjing 210093, China; dzg@nju.edu.cn

Received 2005 June 3; accepted 2005 July 19

ABSTRACT

The prompt localization of GRB 050525A by *Swift* allowed rapid follow-up of the afterglow. The observations revealed that the optical afterglow had a major rebrightening starting at ~ 0.01 days and ending at ~ 0.03 days, which was followed by an initial power-law decay. Here we show that this early emission feature can be interpreted as reverse-shock emission superposed by forward-shock emission in an interstellar medium environment. By fitting the observed data, we further constrain some parameters of the standard fireball-shock model: the initial Lorentz factor of the ejecta $\gamma_0 > 120$, the magnetic energy fraction $\epsilon_B > 4 \times 10^{-6}$, and the medium density $n < 2 \text{ cm}^{-3}$. These limits are consistent with those from other very early optical afterglows observed so far. In principle, a wind environment for GRB 050525A is disfavored.

Subject headings: gamma rays: bursts — relativity — shock waves

1. INTRODUCTION

The gamma-ray burst GRB 050525A is a bright, brief flash of gamma-ray radiation detected by the *Swift* Burst Alert Telescope (BAT) on 2005 May 25 at 00:02:53 (UT; Band et al. 2005). It showed two peaks, with a duration of $T_{90} = 8.8 \pm 0.5$ s in the 15–350 keV band (Markwardt et al. 2005; Cummings et al. 2005). Fitting to the Band spectral model yields a low-energy photon index of $\alpha = 1.0 \pm 0.1$ and a peak energy of $E_p = 79 \pm 4$ keV (Cummings et al. 2005). The fluence in the 15–350 keV band is $(2.0 \pm 0.1) \times 10^{-5} \text{ ergs cm}^{-2}$. This burst was also detected by other instruments, such as *INTEGRAL* (*International Gamma-Ray Astrophysics Laboratory*) and *Konus-Wind*, with peak fluxes of $\sim 3.2 \times 10^{-6} \text{ ergs cm}^{-2} \text{ s}^{-1}$ (Gotz et al. 2005) and $\sim 8.7 \times 10^{-6} \text{ ergs cm}^{-2} \text{ s}^{-1}$ (Golenetskii et al. 2005), respectively. The fluences were $\geq 1.2 \times 10^{-5} \text{ ergs cm}^{-2}$ in 20–200 keV (for a 12 s integration time) by *INTEGRAL* and $\sim 7.8 \times 10^{-5} \text{ ergs cm}^{-2}$ in 20–1000 keV (for a 11.5 s integration time) by *Konus-Wind*. The time-integrated spectrum shows a peak energy $E_p = 84.1 \pm 1.7$ keV by *Konus-Wind* (Golenetskii et al. 2005). About 6 minutes later, the Robotic Optical Transient Search Experiment (ROTSE) III telescope in Namibia was able to obtain images and detected an optical afterglow of 14.7 mag (Rykoﬀ et al. 2005a). A presumed host galaxy was measured with a redshift of $z = 0.606$, based on both [O III] $\lambda 5007$ and H β emission and Ca H and K and Ca I $\lambda 4228$ absorption (Foley et al. 2005). Assuming cosmological parameters $\Omega_M = 0.27$, $\Omega_\Lambda = 0.73$, and $H_0 = 71 \text{ km s}^{-1} \text{ Mpc}^{-1}$, the isotropic-equivalent gamma-ray energy is about $1.2 \times 10^{53} \text{ ergs}$.

The follow-up observations of GRB 050525A revealed that the optical afterglow decayed as $\propto t^{-1.3}$ until about 0.01 days after the burst. Subsequently, the afterglow showed a major rebrightening starting at ~ 0.01 days and ending at ~ 0.03 days and then decayed as $\propto t^{-1.0}$. This early-time emission feature is similar to the behavior of the external reverse-shock emission predicted by the standard fireball-shock model (Mészáros & Rees 1997, 1999; Sari & Piran 1999b), which was first confirmed by the detections of early prompt optical emission from GRB 990123 (Galama et al. 1999; Akerlof et al. 1999; Sari & Piran 1999a). The reverse-shock model was also suggested to

interpret early optical emission of GRB 021004 (Fox et al. 2003b; Kobayashi & Zhang 2003a) and GRB 021211 (Fox et al. 2003a; Li et al. 2003; Wei 2003; Panaitescu & Kumar 2004b). In addition, the prompt optical-infrared emission from GRB 041219A was recently suggested to be internal-shock emission, since a strong correlation between gamma-ray and optical-infrared signals was detected (Vestrand et al. 2005; Blake et al. 2005), which further confirmed the standard internal-external shock model of gamma-ray bursts (GRBs). Mirabal et al. (2005) reported a break at ~ 0.4 days in the optical afterglow light curve of GRB 050525A. In this paper, we show that the optical afterglow in ~ 0.4 days after the *Swift* trigger can be well understood as caused by reverse-shock emission superposed by forward-shock emission.

2. OPTICAL EMISSION FROM FORWARD AND REVERSE SHOCKS

The standard model for GRBs and their afterglows is the fireball-shock model (for recent reviews, see Mészáros 2002; Zhang & Mészáros 2004; Piran 2004). In this model, the prompt emission of GRBs is ascribed to internal shocks and the long-term afterglow to external shocks. The prompt or very early optical emission is therefore explained as a consequence of the reverse component of the external shocks (Mészáros & Rees 1997; Sari & Piran 1999a).

For shock-accelerated slow-cooling electrons with a power-law distribution, the typical spectrum of synchrotron emission is described by three power laws (Sari et al. 1998): (1) $F_\nu = (\nu/\nu_m)^{1/3} F_{\nu, \text{max}}$ for $\nu < \nu_m$, (2) $F_\nu = (\nu/\nu_m)^{-(p-1)/2} F_{\nu, \text{max}}$ for $\nu_m < \nu < \nu_c$, and (3) $F_\nu = (\nu_c/\nu_m)^{-(p-1)/2} (\nu/\nu_c)^{-p/2} F_{\nu, \text{max}}$ for $\nu > \nu_c$, where ν_m , ν_c , and $F_{\nu, \text{max}}$ are the typical synchrotron frequency, cooling frequency, and peak flux, respectively. The parameter p is the index of the electron energy distribution. Here we ignore synchrotron self-absorption because its corresponding frequency may be much less than the optical band of interest.

Both a forward shock and a reverse shock emerge when an ultrarelativistic cold GRB ejecta with initial Lorentz factor of γ_0 sweeps up a stationary cold interstellar medium: the forward shock propagates into the interstellar medium, and the reverse shock propagates back into the ejecta (Katz 1994; Sari & Piran 1995).

The emission of the forward shock is characterized by (Sari et al. 1998)

$$\nu_{m,f} = 4.6 \times 10^{11} \left(\frac{1+z}{2} \right)^{1/2} \left(\frac{E_{\text{iso}}}{10^{53} \text{ ergs}} \right)^{1/2} \left(\frac{\epsilon_B}{10^{-3}} \right)^{1/2} \times \left(\frac{\epsilon_e}{10^{-1}} \right)^2 \left(\frac{g_m}{0.087} \right) t_d^{-3/2} \text{ Hz}, \quad (1)$$

$$\nu_{c,f} = 5.8 \times 10^{16} \left(\frac{1+z}{2} \right)^{-1/2} \left(\frac{E_{\text{iso}}}{10^{53} \text{ ergs}} \right)^{-1/2} \left(\frac{\epsilon_B}{10^{-3}} \right)^{-3/2} \times \left(\frac{g_c}{0.128} \right) n^{-1} t_d^{-1/2} \text{ Hz}, \quad (2)$$

$$t_{m,f} = 1.1 \times 10^{-2} \left(\frac{1+z}{2} \right)^{1/3} \left(\frac{E_{\text{iso}}}{10^{53} \text{ ergs}} \right)^{1/3} \left(\frac{\epsilon_B}{10^{-3}} \right)^{1/3} \times \left(\frac{\epsilon_e}{10^{-1}} \right)^{4/3} \left(\frac{g_m}{0.087} \right)^{2/3} \left(\frac{\nu_R}{10^{15} \text{ Hz}} \right)^{-2/3} \text{ days}, \quad (3)$$

$$F_{\nu, \text{max}, f} = 25 \left(\frac{1+z}{2} \right) \left(\frac{E_{\text{iso}}}{10^{53} \text{ ergs}} \right) \left(\frac{\epsilon_B}{10^{-3}} \right)^{1/2} \times \left(\frac{D_L}{10^{28} \text{ cm}} \right)^{-2} \left(\frac{g_{\text{max}}}{2.44} \right) n^{1/2} \text{ mJy}, \quad (4)$$

where $t_{m,f}$ are the critical times when the break frequency, $\nu_{m,f}$, crosses the observed frequency ν_R , ϵ_B is the fraction of the shock energy that goes into the magnetic field, ϵ_e is the fraction of the shock energy that goes into the electrons, $g_m = (p - 0.67)(p - 2)^2/(p - 1)^2$, $g_c = (p - 0.46)e^{-1.16p}$, $g_{\text{max}} = p + 0.14$ (Granot & Sari 2002), E_{iso} is the isotropic-equivalent kinetic energy, n is the density of the interstellar medium in units of 1 cm^{-3} , z is the redshift of the burst, D_L is the corresponding luminosity distance, and t_d is the observer's time in units of 1 day. The above equations are valid for $p > 2$. Afterglows with hard electron spectra of $1 < p < 2$ have been discussed by Dai & Cheng (2001).

For reverse shocks, it is possible to get a simple analytic solution in two limiting cases: thin shell and thick shell (which correspond to Newtonian and relativistic reverse shocks, respectively; Sari & Piran 1995). Since the reverse-shocked gas is separated from the forward-shocked gas by a contact discontinuity, which keeps the equality of pressures and velocities in both shocks, we can find the emission properties of the reverse shock with the aid of the correlations between the forward and reverse shocks at crossing time t_\times (Kobayashi 2000; Kobayashi & Zhang 2003a). First, since the reverse- and forward-shocked gases have the same magnetic field and Lorentz factor at t_\times , the cooling frequency of the reverse-shocked electrons is equal to that of the forward-shocked electrons, $\nu_{c,r}(t_\times) = \nu_{c,f}(t_\times)$. Second, the electron's random Lorentz factor of the reverse shock is smaller than that of the forward shock by a factor of γ_0/γ_\times (where γ_\times is the Lorentz factor of both shocked regions at t_\times), and the typical synchrotron frequency of the reverse shock is a factor of $\gamma_0^2/\gamma_\times^4$ less than that of the forward shock, $\nu_{m,r}(t_\times) = (\gamma_0^2/\gamma_\times^4)\nu_{m,f}(t_\times)$. This is basically valid for the thick-shell case. As for a thin shell, it is more realistic with the expression $\nu_{m,r}(t_\times) = (\gamma_{34,\times} - 1)^2/(\gamma_\times - 1)^2 \nu_{m,f}(t_\times)$, where $\gamma_{34,\times} \simeq (\gamma_\times/\gamma_0 + \gamma_0/\gamma_\times)/2$ is the Lorentz factor of the shocked ejecta in the rest frame comoving with the unshocked ejecta at the crossing time and $\gamma_\times \simeq \gamma_0/2$ (Zhang et al. 2003; Fan & Wei 2005). Third, the peak flux $F_{\nu, \text{max}}$ of an emission region is proportional to the electron number, the magnetic field, and the Lorentz boost. Since at t_\times the electron number of the ejected shell is larger than that of the swept-up medium by a factor of γ_\times^2/γ_0 , we

obtain $F_{\nu, \text{max}, r}(t_\times) = (\gamma_\times^2/\gamma_0)F_{\nu, \text{max}, f}(t_\times)$. Therefore, we can directly write down the corresponding characteristic variables of the reverse-shock emission, at $t = t_\times$,

$$\nu_{m,r}(t_\times) = 4.6 \times 10^{11} \left(\frac{1+z}{2} \right)^{-1} \left(\frac{\epsilon_e}{10^{-1}} \right)^2 \left(\frac{\epsilon_B}{10^{-3}} \right)^{1/2} n^{1/2} \times \left(\frac{g_m}{0.087} \right) \left(\frac{\gamma_0}{10^{2.5}} \right)^2 \text{ Hz}, \quad (5)$$

$$\nu_{c,r}(t_\times) = 2.8 \times 10^{18} \left(\frac{1+z}{2} \right)^{-1} \left(\frac{E_{\text{iso}}}{10^{53} \text{ ergs}} \right)^{-2/3} \times \left(\frac{\epsilon_B}{10^{-3}} \right)^{-3/2} n^{-5/6} \left(\frac{g_c}{0.128} \right) \left(\frac{\gamma_0}{10^{2.5}} \right)^{4/3} \text{ Hz}, \quad (6)$$

$$F_{\nu, \text{max}, r}(t_\times) = 10 \left(\frac{1+z}{2} \right) \left(\frac{\epsilon_B}{10^{-3}} \right)^{1/2} n^{1/2} \left(\frac{E_{\text{iso}}}{10^{53} \text{ ergs}} \right) \times \left(\frac{D_L}{10^{28} \text{ cm}} \right)^{-2} \left(\frac{g_{\text{max}}}{2.44} \right) \left(\frac{\gamma_0}{10^{2.5}} \right) \text{ Jy} \quad (7)$$

for the thin-shell (i.e., Newtonian) case, and

$$\nu_{m,r}(T) = 5.1 \times 10^{11} \left(\frac{1+z}{2} \right)^{-1} \left(\frac{\epsilon_e}{10^{-1}} \right)^2 \left(\frac{\epsilon_B}{10^{-3}} \right)^{1/2} n^{1/2} \times \left(\frac{g_m}{0.087} \right) \left(\frac{\gamma_0}{10^{2.5}} \right)^2 \text{ Hz}, \quad (8)$$

$$\nu_{c,r}(T) = 1.7 \times 10^{18} \left(\frac{1+z}{2} \right)^{-1/2} \left(\frac{\epsilon_B}{10^{-3}} \right)^{-3/2} n^{-1} \times \left(\frac{E_{\text{iso}}}{10^{53} \text{ ergs}} \right)^{-1/2} \left(\frac{g_c}{0.128} \right) \left(\frac{T}{10^2 \text{ s}} \right)^{-1/2} \text{ Hz}, \quad (9)$$

$$F_{\nu, \text{max}, r}(T) = 2.3 \left(\frac{1+z}{2} \right)^{7/4} \left(\frac{E_{\text{iso}}}{10^{53} \text{ ergs}} \right)^{5/4} \times \left(\frac{\epsilon_B}{10^{-3}} \right)^{1/2} n^{1/4} \left(\frac{g_{\text{max}}}{2.44} \right) \left(\frac{D_L}{10^{28} \text{ cm}} \right)^{-2} \times \left(\frac{T}{10^2 \text{ s}} \right)^{-3/4} \left(\frac{\gamma_0}{10^{2.5}} \right)^{-1} \text{ Jy} \quad (10)$$

for the thick-shell (i.e., relativistic) case. Here the GRB duration T is given by the shell width Δ_0/c , according to the internal-shock model. As derived by Sari & Piran (1999b) and Kobayashi (2000), the typical synchrotron frequency and peak flux evolve as $\nu_{m,r} \propto t^6$, $F_{\nu, \text{max}, r} \propto t^{3/2}$ at $t < t_\times$ and $\nu_{m,r} \propto t^{-54/35}$, $F_{\nu, \text{max}, r} \propto t^{-34/35}$ at $t > t_\times$ for the thin-shell case, and $\nu_{m,r} = \text{constant}$, $F_{\nu, \text{max}, r} \propto t^{1/2}$ at $t < T$ and $\nu_{m,r} \propto t^{-73/48}$, $F_{\nu, \text{max}, r} \propto t^{-47/48}$ at $t > T$ for the thick-shell case. Before the crossing time, the cooling frequency evolves as $\nu_{c,r} \propto t^{-2}$ for the thin-shell case and $\nu_{c,r} \propto t^{-1}$ for the thick-shell case; after the crossing time, $\nu_{c,r}$ turns into the cutoff frequency due to synchrotron cooling of electrons without acceleration, and it evolves the same as $\nu_{m,r}$ for both cases. According to the emission properties shown above, we derive light curves of the emission from the forward- and reverse-shocked regions and thus can constrain the model parameters by fitting the early afterglow of GRB 050525A.

3. CONSTRAINTS ON PARAMETERS OF GRB 050525A

From the emission features described by equations (1), (2), (5), (6), (8), and (9), we see that the optical band is commonly between the typical frequency ν_m and cooling frequency ν_c in

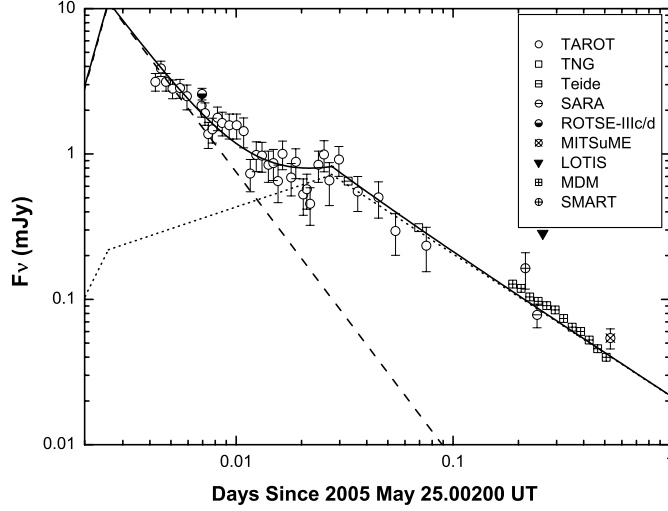


FIG. 1.—*R*-band afterglow light curve of GRB 050525A. The fitting curve (solid line) is generated by superposition of the forward-shock emission (dotted line) and reverse-shock emission (dashed line) with $\epsilon_B = 0.0025$, $\epsilon_e = 0.2$, $n = 0.003 \text{ cm}^{-3}$, $E_{\text{iso}} = 10^{53} \text{ ergs}$, $p = 2.3$, and $\gamma_0 = 200$. These values are basically consistent with the thin-shell case. Data are taken from the GRB Coordinates Network (GCN; Malesani et al. 2005; Klotz et al. 2005a, 2005b; Torii & BenDaniel 2005; Homewood et al. 2005; Rykoff et al. 2005b; Yanagisawa et al. 2005; Milne et al. 2005; Mirabal et al. 2005; Cobb & Bailyn 2005).

both forward and reverse shocks around the crossing time. Thus, the optical light curve of GRB 050525A can be fitted by the superposition of two broken power laws: (1) $F_{\nu,f} \propto t_d^{1/2}$ for $t_d < t_{m,f}$ and $F_{\nu,f} \propto t_d^{(3-p)/4}$ for $t_d > t_{m,f}$ for the forward shock and (2) $F_{\nu,r} \propto t_d^{(2p-1)/2}$ for $t_d < t_x$ and $F_{\nu,r} \propto t_d^{(-27p+7)/35}$ for $t_d > t_x$ for the reverse shock. These scaling laws are valid for the thin-shell case, in which the reverse shock decelerates the shell insignificantly (Kobayashi 2000).

In Figure 1 we present the *R*-band afterglow light curve of GRB 050525A between May 25.0062 UT ($\Delta t \approx 0.004$ days) and May 25.5333 UT ($\Delta t \approx 0.531$ days). We find that $t_{m,f} \approx 0.027$ days, $F_{\nu,\text{max},f} \approx 0.719$ mJy, and $p \approx 2.3$ can fit the light curve well for the component of forward-shock emission. Given redshift $z = 0.606$ (Foley et al. 2005), the corresponding luminosity distance is $D_L = 1.1 \times 10^{28} \text{ cm}$. Using equations (3) and (4), we obtain

$$\epsilon_e \approx 8.3n^{1/4} \left(\frac{E_{\text{iso}}}{10^{53} \text{ ergs}} \right)^{1/4} \quad (11)$$

and

$$\epsilon_B \approx 1.0 \times 10^{-5} n^{-1} \left(\frac{E_{\text{iso}}}{10^{53} \text{ ergs}} \right)^{-2}. \quad (12)$$

Furthermore, from the flux inferred from the light curve of the reverse-shock emission (Fig. 1, dashed line, where we see a flux $F_{\nu,r} = 0.75$ mJy at $t = 0.01$ days), using equations (5) and (7), we further obtain

$$\left(\frac{E_{\text{iso}}}{10^{53} \text{ ergs}} \right)^{1.658} \left(\frac{\epsilon_B}{10^{-3}} \right)^{0.825} \left(\frac{\epsilon_e}{10^{-1}} \right)^{1.3} n^{0.167} \left(\frac{\gamma_0}{10^{2.5}} \right)^{-2.965} \approx 5.9. \quad (13)$$

By simple algebra, from equations (11)–(13) we obtain a constraint on the initial Lorentz factor of GRB ejecta,

$$\gamma_0 = 121 \left(\frac{E_{\text{iso}}}{10^{53} \text{ ergs}} \right)^{0.112} \left(\frac{n}{1 \text{ cm}^{-3}} \right)^{-0.112}, \quad (14)$$

which is weakly dependent on the isotropic-equivalent kinetic energy E_{iso} and interstellar medium density n . Assuming the efficiency of energy conversion is $\eta = 0.5$, E_{iso} is approximately equal to the detected isotropic-equivalent gamma-ray energy, i.e., $1.2 \times 10^{53} \text{ ergs}$. Thus, we can obtain a mutual constraint between ϵ_B and ϵ_e from equations (11) and (12). By eliminating the medium density n , we have $\epsilon_B = 4 \times 10^{-6} \epsilon_e^{-4}$. Moreover, as a natural consequence of $\epsilon_e < 1$, we have $\gamma_0 > 116$, $\epsilon_B > 4 \times 10^{-6}$, and $n < 2 \text{ cm}^{-3}$. These constraints are more clear than the cases of GRB 990123 (Sari & Piran 1999a), GRB 021004 (Kobayashi & Zhang 2003a), and GRB 021211 (Wei 2003). Our preliminary fit to the afterglow observations of GRB 050525A updated to May 25.5333 UT ($\Delta t \approx 0.531$ days) is shown in Figure 1.

In addition, we also give a constraint on the parameters for the thick-shell case. We find, from a fit similar to that shown above, that the crossing time of the reverse shock, i.e., the GRB duration T , is approximated by

$$T \approx 553 \left(\frac{E_{\text{iso}}}{10^{53} \text{ ergs}} \right)^{0.06} \left(\frac{n}{1 \text{ cm}^{-3}} \right)^{-0.06} \left(\frac{\gamma_0}{10^{2.5}} \right)^{0.25} \text{ s}, \quad (15)$$

which is inconsistent with the observed $T_{90} \approx 10$ s (Markwardt et al. 2005; Gotz et al. 2005). This implies that GRB 050525A seems to be a thin-shell case.

4. DISCUSSION AND CONCLUSIONS

The optical afterglow of GRB 050525A rebrightened starting at ~ 0.01 days and ending at ~ 0.03 days, which was followed by an initial power-law decay. In this paper, we have shown that this early emission feature can be interpreted as the reverse-shock emission superposed by the forward-shock emission in an interstellar medium environment. A good fit to the observed light curve is shown in Figure 1. We further find the initial Lorentz factor of the ejecta $\gamma_0 > 120$. Some other model parameters are also constrained: the magnetic energy fraction $\epsilon_B > 4 \times 10^{-6}$ and the medium density $n < 2 \text{ cm}^{-3}$. These limits are consistent with those from the other very early optical afterglows observed so far (Sari & Piran 1999a; Kobayashi & Zhang 2003a; Wei 2003; Panaitescu & Kumar 2004b; Nakar & Piran 2005) and with the values of the forward-shock parameters (Panaitescu & Kumar 2001).

Our model is simplified under some assumptions. First, the reverse- and forward-shocked regions have the same electron and magnetic energy fractions, requiring that the ejecta is not initially magnetized. This requirement seems to be relaxed for GRB 990123 (Fan et al. 2002; Zhang et al. 2003). The interaction of a magnetized ejecta with its surrounding medium has been investigated in detail (Fan et al. 2004; Zhang & Kobayashi 2005). Second, we neglect the effect of inverse Compton scattering (ICS) on the reverse-shock emission in § 2. As shown by Wang et al. (2001a, 2001b), this effect not only decreases the cooling frequency but also produces higher energy emission. However, this decrease does not affect the limits derived above because the cooling frequency is much larger than the optical band at the times of our interest. Third, the surrounding environment is assumed to be a uniform interstellar medium, in which case two types of light curves are expected for the reverse-forward shock emission combination: a rebrightening light curve (type I) and a flattening light curve (type II; Zhang et al. 2003). Early afterglows in wind environments have been studied by Chevalier & Li (2000), Wu et al. (2003), Kobayashi & Zhang (2003b), Panaitescu & Kumar (2004b), and Zou et al. (2005). Generally, a flattening light curve in the optical band is expected in the wind model

(Kobayashi & Zhang 2003b; Zou et al. 2005), i.e., there is only a type II light curve for the reverse-forward shock emission combination. Since the early optical afterglow of GRB 050525A shows a rebrightening (type I) light curve, the reverse-forward shock model in a wind environment for the early afterglow of GRB 050525A is not favored.

The observed break at $t_j \simeq 0.4$ days in the optical afterglow light curve of GRB 050525A (Mirabal et al. 2005) may be due to an ultrarelativistic jet. This conclusion seems to be strengthened by Lulin Observatory around 17.7 hr after the burst (at which the R -band magnitude is about 21.3 ± 0.1 ; Chiang et al. 2005). If so, the jet's half-opening angle $\theta = 0.051(t_j/0.4 \text{ days})^{3/8}(E_{\text{iso}}/10^{53} \text{ ergs})^{-1/8}(n/0.1 \text{ cm}^{-3})^{1/8}(\eta_\gamma/0.5)^{1/8}$ (Sari et al. 1999), and thus the beaming-corrected gamma-ray energy $E_{\text{jet}} = 1.3 \times 10^{50} (t_j/0.4 \text{ days})^{3/4}(E_{\text{iso}}/10^{53} \text{ ergs})^{3/4}(n/0.1 \text{ cm}^{-3})^{1/4}(\eta_\gamma/0.5)^{1/4} \text{ ergs}$, which is a factor of a few smaller than the mean energy release found by Frail et al. (2001) for $n \sim 0.1 \text{ cm}^{-3}$ and $\eta_\gamma \sim 0.5$. Even so, this energy still satisfies the relation of Ghirlanda et al. (2004), $E_{\text{jet}}/10^{50} \text{ ergs} = (1.12 \pm 0.12)[(1+z)E_p/100 \text{ keV}]^{1.50 \pm 0.08}$ (see Dai et al. 2004).

Finally, we want to point out that besides the reverse-shock model discussed in this paper, the other plausible explanations for a rebrightening light curve include a density-jump medium (Dai & Lu 2002; Lazzati et al. 2002), pure Poynting flux injection (Dai & Lu 1998), baryon-dominated injection (Rees & Mészáros 1998; Granot et al. 2003; Nakar et al. 2003; Björnsson et al. 2004), a two-component jet (Berger et al. 2003; Huang et al. 2004), a neutron-fed fireball (Beloborodov 2003), temporal fluctuation of ϵ_e and/or ϵ_B , and departure of the electron distribution from a power law (Panaitescu & Kumar 2004a). Multiwavelength observations in the *Swift* era are expected to distinguish among these possibilities.

We thank Y. Z. Fan and L. J. Gou for constructive comments, X. F. Wu and Y. C. Zou for helpful discussions, and Y. F. Huang and X. Y. Wang for a careful reading of our manuscript. This work was supported by the National Natural Science Foundation of China (grants 10233010 and 10221001) and the Ministry of Science and Technology of China (NKBRF G19990754).

REFERENCES

- Akerlof, C., et al. 1999, *Nature*, 398, 400
 Band, D., et al. 2005, *GCN Circ.* 3466, <http://gcn.gsfc.nasa.gov/gcn/gcn3/3466.gcn3>
 Beloborodov, A. M. 2003, *ApJ*, 585, L19
 Berger, E., et al. 2003, *Nature*, 426, 154
 Björnsson, G., Gudmundsson, E. H., & Johanesson, G. 2004, *ApJ*, 615, L77
 Blake, C. H., et al. 2005, *Nature*, 435, 181
 Chevalier, R. A., & Li, Z. Y. 2000, *ApJ*, 536, 195
 Chiang, P. S., Huang, K. Y., Ip, W. H., Urata, Y., Qiu, Y., & Lou, Y. Q. 2005, *GCN Circ.* 3486, <http://gcn.gsfc.nasa.gov/gcn/gcn3/3486.gcn3>
 Cobb, B. E., & Baily, C. D. 2005, *GCN Circ.* 3506, <http://gcn.gsfc.nasa.gov/gcn/gcn3/3506.gcn3>
 Cummings, J., et al. 2005, *GCN Circ.* 3479, <http://gcn.gsfc.nasa.gov/gcn/gcn3/3479.gcn3>
 Dai, Z. G., & Cheng, K. S. 2001, *ApJ*, 558, L109
 Dai, Z. G., Liang, E. W., & Xu, D. 2004, *ApJ*, 612, L101
 Dai, Z. G., & Lu, T. 1998, *Phys. Rev. Lett.*, 81, 4301
 ———. 2002, *ApJ*, 565, L87
 Fan, Y. Z., Dai, Z. G., Huang, Y. F., & Lu, T. 2002, *Chinese J. Astron. Astrophys.*, 2, 449
 Fan, Y. Z., & Wei, D. M. 2005, *MNRAS*, in press (astro-ph/0506155)
 Fan, Y. Z., Wei, D. M., & Wang, C. F. 2004, *A&A*, 424, 477
 Foley, R. J., Chen, H. W., Bloom, J., & Prochaska, J. X. 2005, *GCN Circ.* 3483, <http://gcn.gsfc.nasa.gov/gcn/gcn3/3483.gcn3>
 Fox, D. W., et al. 2003a, *ApJ*, 586, L5
 ———. 2003b, *Nature*, 422, 284
 Frail, D. A., et al. 2001, *ApJ*, 562, L55
 Galama, T. J., et al. 1999, *Nature*, 398, 394
 Ghirlanda, G., Ghisellini, G., & Lazzati, D. 2004, *ApJ*, 616, 331
 Golenetskii, S., Aptekar, R., Mazets, E., Pal'Shin, V., Frederiks, D., & Cline, T. 2005, *GCN Circ.* 3474, <http://gcn.gsfc.nasa.gov/gcn/gcn3/3474.gcn3>
 Gotz, D., Mereghetti, S., Mowlavi, N., Shaw, S., Beck, M., Borkowski, J., & Lund, N. 2005, *GCN Circ.* 3472, <http://gcn.gsfc.nasa.gov/gcn/gcn3/3472.gcn3>
 Granot, J., Nakar, E., & Piran, T. 2003, *Nature*, 426, 138
 Granot, J., & Sari, R. 2002, *ApJ*, 568, 820
 Homewood, A., Hartmann, D. H., Garimella, K., Henson, G., McLaughlin, J., & Brimeyer, A. 2005, *GCN Circ.* 3491, <http://gcn.gsfc.nasa.gov/gcn/gcn3/3491.gcn3>
 Huang, Y. F., Wu, X. F., Dai, Z. G., Ma, H. T., & Lu, T. 2004, *ApJ*, 605, 300
 Katz, J. I. 1994, *ApJ*, 422, 248
 Klotz, A., Boër, M., & Atteia, J. L. 2005a, *GCN Circ.* 3473, <http://gcn.gsfc.nasa.gov/gcn/gcn3/3473.gcn3>
 Klotz, A., Boër, M., Atteia, J. L., Stratta, G., Behrend, R., Malacrino, F., & Damerjji, Y. 2005b, *A&A*, 439, L35
 Kobayashi, S. 2000, *ApJ*, 545, 807
 Kobayashi, S., & Zhang, B. 2003a, *ApJ*, 582, L75
 Kobayashi, S., & Zhang, B. 2003b, *ApJ*, 597, 455
 Lazzati, D., Rossi, E., Covino, S., Ghisellini, G., & Malesani, D. 2002, *A&A*, 396, L5
 Li, W., Filippenko, A. V., Chornock, R., & Jha, S. 2003, *ApJ*, 586, L9
 Malesani, D., Piranomonte, S., Fiore, F., Tagliaferri, G., Fugazza, D., & Cosentino, R. 2005, *GCN Circ.* 3469, <http://gcn.gsfc.nasa.gov/gcn/gcn3/3469.gcn3>
 Markwardt, C., et al. 2005, *GCN Circ.* 3467, <http://gcn.gsfc.nasa.gov/gcn/gcn3/3467.gcn3>
 Mészáros, P. 2002, *ARA&A*, 40, 137
 Mészáros, P., & Rees, M. J. 1997, *ApJ*, 476, 232
 ———. 1999, *MNRAS*, 306, L39
 Milne, P. A., Williams, G. G., & Park, H.-S. 2005, *GCN Circ.* 3485, <http://gcn.gsfc.nasa.gov/gcn/gcn3/3485.gcn3>
 Mirabal, N., Bonfield, D., & Schawinski, K. 2005, *GCN Circ.* 3488, <http://gcn.gsfc.nasa.gov/gcn/gcn3/3488.gcn3>
 Nakar, E., & Piran, T. 2005, *ApJ*, 619, L147
 Nakar, E., Piran, T., & Granot, J. 2003, *NewA*, 8, 495
 Panaitescu, A., & Kumar, P. 2001, *ApJ*, 560, L49
 ———. 2004a, *MNRAS*, 350, 213
 ———. 2004b, *MNRAS*, 353, 511
 Piran, T. 2004, *Rev. Mod. Phys.*, 76, 1143
 Rees, M., & Mészáros, P. 1998, *ApJ*, 496, L1
 Rykoff, E. S., Yost, S. A., & Swan, H. 2005a, *GCN Circ.* 3465, <http://gcn.gsfc.nasa.gov/gcn/gcn3/3465.gcn3>
 Rykoff, E. S., Yost, S. A., Swan, H., & Quimby, R. 2005b, *GCN Circ.* 3468, <http://gcn.gsfc.nasa.gov/gcn/gcn3/3468.gcn3>
 Sari, R., & Piran, T. 1995, *ApJ*, 455, L143
 ———. 1999a, *ApJ*, 517, L109
 ———. 1999b, *ApJ*, 520, 641
 Sari, R., Piran, T., & Halpern, J. P. 1999, *ApJ*, 519, L17
 Sari, R., Piran, T., & Narayan, R. 1998, *ApJ*, 497, L17
 Torii, K., & BenDaniel, M. 2005, *GCN Circ.* 3470, <http://gcn.gsfc.nasa.gov/gcn/gcn3/3470.gcn3>
 Vestrand, W. T., et al. 2005, *Nature*, 435, 178
 Wang, X. Y., Dai, Z. G., & Lu, T. 2001a, *ApJ*, 546, L33
 ———. 2001b, *ApJ*, 556, 1010
 Wei, D. M. 2003, *A&A*, 402, L9
 Wu, X. F., Dai, Z. G., Huang, Y. F., & Lu, T. 2003, *MNRAS*, 342, 1131
 Yanagisawa, K., Toda, H., & Kawai, N. 2005, *GCN Circ.* 3489, <http://gcn.gsfc.nasa.gov/gcn/gcn3/3489.gcn3>
 Zhang, B., & Kobayashi, S. 2005, *ApJ*, 628, 315
 Zhang, B., Kobayashi, S., & Mészáros, P. 2003, *ApJ*, 595, 950
 Zhang, B., & Mészáros, P. 2004, *Int. J. Mod. Phys. A*, 19, 2385
 Zou, Y. C., Wu, X. F., & Dai, Z. G. 2005, *MNRAS*, in press